Research Article | Vol. 25, No. 25 | 11 Dec 2017 | OPTICS EXPRESS 31377
Optics EXPRESS

1.4 µm continuous-wave diamond Raman laser

RICCARDO CASULA,[1,*] JUSSI-PEKKA PENTTINEN,[2] ALAN J. KEMP,[1] MIRCEA GUINA,[2] AND JENNIFER E. HASTIE[1]

[1]*Institute of Photonics, Department of Physics, University of Strathclyde, Technology and Innovation Centre, 99 George Street, Glasgow G1 1RD, UK*
[2]*Optoelectronic Research Centre, Tampere University of Technology, Korkeakoulunkatu 3, Tampere FIN-33101, Finland*
**riccardo.casula@strath.ac.uk*

Abstract: The longest wavelength (~1.4 µm) emitted by a diamond Raman laser pumped by a semiconductor disk laser (SDL) is reported. The output power of the intracavity-pumped Raman laser reached a maximum of 2.3 W with an optical conversion efficiency of 3.4% with respect to the absorbed diode pump power. Narrow Stokes emission (FWHM <0.1 nm) was attained using etalons to limit the fundamental spectrum to a single etalon peak. Tuning of the Raman laser over >40 nm was achieved via rotation of an intracavity birefringent filter that tuned the SDL oscillation wavelength.

OCIS codes: (140.3550) Lasers, Raman; (140.3580) Solid-state laser; (140.3600) Tunable lasers; (140.7270) Vertical emitting lasers.

References and links

1. H. M. Pask, "The design and operation of solid-state Raman lasers," Prog. Quantum Electron. **27**, 3–56 (2003).
2. D. C. Parrotta, A. J. Kemp, M. D. Dawson, and J. E. Hastie, "Multiwatt, Continuous-Wave, Tunable Diamond Raman Laser With Intracavity Frequency-Doubling to the Visible Region," IEEE J. Sel. Top. Quantum Electron. **19**, 1400108 (2013).
3. O. Lux, S. Sarang, R. J. Williams, A. McKay, and R. P. Mildren, "Single longitudinal mode diamond Raman laser in the eye-safe spectral region for water vapor detection," Opt. Express **24**(24), 27812–27820 (2016).
4. M. Kuznetsov, F. Hakimi, R. Sprague, and A. Mooradian, "Design and characteristics of high-power (<0.5-W CW) diode-pumped vertical-external-cavity surface-emitting semiconductor lasers with circular TEM_{00} beams," IEEE J. Sel. Top. Quantum Electron. **5**, 561–573 (1999).
5. D. C. Parrotta, W. Lubeigt, A. J. Kemp, D. Burns, M. D. Dawson, and J. E. Hastie, "Continuous-wave Raman laser pumped within a semiconductor disk laser cavity," Opt. Lett. **36**(7), 1083–1085 (2011).
6. N. Schulz, J. M. Hopkins, M. Rattunde, D. Burns, and J. Wagner, "High-brightness long-wavelength semiconductor disk lasers," Laser Photonics Rev. **2**(3), 160–181 (2008).
7. S. Calvez, J. E. Hastie, M. Guina, O. G. Okhotnikov, and M. D. Dawson, "Semiconductor disk lasers for the generation of visible and ultraviolet radiation," Laser Photonics Rev. **3**(5), 407–434 (2009).
8. B. Heinen, T.-L. Wang, M. Sparenberg, A. Weber, B. Kunert, J. Hader, S. W. Koch, J. V. Moloney, M. Koch, and W. Stolz, "106 W continuous-wave output power from vertical-external-cavity surface-emitting laser," Electron. Lett. **48**(9), 516 (2012).
9. S. Ranta, M. Tavast, T. Leinonen, N. Van Lieu, G. Fetzer, and M. Guina, "1180 nm VECSEL with output power beyond 20 W," Electron. Lett. **49**(1), 59–60 (2013).
10. E. Kantola, T. Leinonen, S. Ranta, M. Tavast, and M. Guina, "High-efficiency 20 W yellow VECSEL," Opt. Express **22**(6), 6372–6380 (2014).
11. J.-M. Hopkins, S. A. Smith, C. W. Jeon, H. D. Sun, D. Burns, S. Calvez, M. D. Dawson, T. Jouthi, and M. Pessa, "0.6W CW GaInNAs vertical external-cavity surface emitting laser operating at 1.32 µm," Electron. Lett. **40**(1), 30–31 (2004).
12. J. Lyytikäinen, J. Rautiainen, L. Toikkanen, A. Sirbu, A. Mereuta, A. Caliman, E. Kapon, and O. G. Okhotnikov, "1.3-µm optically-pumped semiconductor disk laser by wafer fusion," Opt. Express **17**(11), 9047–9052 (2009).
13. A. Sirbu, N. Volet, A. Mereuta, J. Lyytikäinen, J. Rautiainen, O. Okhotnikov, J. Walczak, M. Wasiak, T. Czyszanowski, A. Caliman, Q. Zhu, V. Iakovlev, and E. Kapon, "Wafer-Fused Optically Pumped VECSELs Emitting in the 1310-nm and 1550-nm Wavebands," Adv. Opt. Technol. **2011**, 1–8 (2011).
14. D. C. Parrotta, R. Casula, J. Penttinen, T. Leinonen, A. J. Kemp, M. Guina, and J. E. Hastie, "InGaAs-QW VECSEL emitting >1300-nm via intracavity Raman conversion," in *SPIE LASE*, K. G. Wilcox, ed. (2016), p. 97340O.
15. W. Lubeigt, G. M. Bonner, J. E. Hastie, M. D. Dawson, D. Burns, and A. J. Kemp, "An intra-cavity Raman laser

#308319 https://doi.org/10.1364/OE.25.031377
Journal © 2017 Received 29 Sep 2017; revised 16 Nov 2017; accepted 21 Nov 2017; published 1 Dec 2017

Optics EXPRESS

using synthetic single-crystal diamond," Opt. Express **18**(16), 16765–16770 (2010).
16. V. G. Savitski, S. Reilly, and A. J. Kemp, "Steady-state raman gain in diamond as a function of pump wavelength," IEEE J. Quantum Electron. **49**(2), 218–223 (2013).
17. R. J. Williams, D. J. Spence, O. Lux, and R. P. Mildren, "High-power continuous-wave Raman frequency conversion from 1.06 μm to 1.49 μm in diamond," Opt. Express **25**(2), 749–757 (2017).
18. R. Loudon, "The Raman effect in crystals," Adv. Phys. **13**(52), 423–482 (1964).
19. A. Sabella, J. A. Piper, and R. P. Mildren, "1240 nm diamond Raman laser operating near the quantum limit," Opt. Lett. **35**(23), 3874–3876 (2010).
20. K. C. Lee, B. J. Sussman, J. Nunn, V. O. Lorenz, K. Reim, D. Jaksch, I. A. Walmsley, P. Spizzirri, and S. Prawer, "Comparing phonon dephasing lifetimes in diamond using Transient Coherent Ultrafast Phonon Spectroscopy," Diamond Related Materials **19**(10), 1289–1295 (2010).
21. G. M. Bonner, J. Lin, A. J. Kemp, J. Wang, H. Zhang, D. J. Spence, and H. M. Pask, "Spectral broadening in continuous-wave intracavity Raman lasers," Opt. Express **22**(7), 7492–7502 (2014).
22. D. J. Spence, "Spatial and Spectral Effects in Continuous-Wave Intracavity Raman Lasers," IEEE J. Sel. Top. Quantum Electron. **21**(1), 134–141 (2015).
23. J. A. Piper and H. M. Pask, "Crystalline Raman Lasers," IEEE J. Sel. Top. Quantum Electron. **13**(3), 692–704 (2007).
24. H. Jasbeer, R. J. Williams, O. Kitzler, A. McKay, S. Sarang, J. Lin, and R. P. Mildren, "Birefringence and piezo-Raman analysis of single crystal CVD diamond and effects on Raman laser performance," J. Opt. Soc. Am. B **33**(3), 56–64 (2016).
25. I. Friel, S. L. Clewes, H. K. Dhillon, N. Perkins, D. J. Twitchen, and G. A. Scarsbrook, "Control of surface and bulk crystalline quality in single crystal diamond grown by chemical vapour deposition," Diamond Related Materials **18**(5–8), 808–815 (2009).
26. D. Welford and M. A. Jaspan, "Single-frequency operation of a Cr:YAG laser from 1332 to 1554 nm," J. Opt. Soc. Am. B **21**(12), 2137–2141 (2004).
27. D. C. Parrotta, A. J. Kemp, M. D. Dawson, and J. E. Hastie, "Tunable continuous-wave diamond Raman laser," Opt. Express **19**(24), 24165–24170 (2011).
28. A. Sennaroglu, C. R. Pollock, and H. Nathel, "Efficient continuous-wave chromium-doped YAG laser," J. Opt. Soc. Am. B **12**(5), 930 (1995).

1. Introduction

Raman lasers use stimulated Raman scattering to down-convert the emission frequency of the pump laser, with an energy difference fixed by the Raman medium, thus extending the spectral coverage of solid-state lasers. In contrast to optical parametric oscillators (OPOs) crystalline Raman lasers are not generally broadly tunable, at least directly. Rather, tuning is achieved via tuning of the pump laser. Compared with OPOs, Raman laser technology is less complex and does not require management of phase matching. Broadly tunable, high-finesse, solid-state Raman laser systems can be pumped with conventional solid-state and thin-disk lasers [1,2], and could potentially enable a wide range of remote gas sensing applications, especially at wavelengths >1.4 μm [3].

Semiconductor disk lasers (SDLs), also known as vertical-external-cavity surface-emitting-lasers (VECSELs) [4], are very attractive pump sources for Raman lasers as the extended cavity of the SDL allows the incorporation of the Raman active crystal and resonator and the fundamental wavelength is broadly tunable [2,5]. Raman conversion offers efficient operation at wavelengths that are otherwise difficult to achieve from an SDL directly.

The SDL gain structure consists of multiple quantum wells (QWs), spaced for resonant periodic gain with emission vertical to the epitaxial plane [4], and is usually deposited directly on top of a distributed Bragg reflector (DBR). With selection of the appropriate lattice-matched III-V semiconductors and the use of bandgap and strain engineering, broad spectral coverage has been achieved with direct emission demonstrated from the visible to the mid-infrared, in the pulsed or continuous-wave (CW) regime [6,7]. SDLs based on InGaAs QWs are the most established and are routinely demonstrated to emit multi-watt CW power at wavelengths between 920 and 1180 nm by varying the indium content in the QWs [8–10].

SDLs with direct emission >1200 nm have been demonstrated either by incorporating nitrogen in the InGaAs lattice (i.e. GaInNAs QWs [11]) or using gain regions based on InAlGaAs/InP QWs which, lacking a lattice-matched material suitable for high quality DBRs, are bonded to separately-grown mirrors via wafer fusion [12]. Sirbu et al. developed wafer-

Optics EXPRESS

fused InAlGaAs SDLs emitting several watts at ~1300, 1480, and 1550 nm [13] but their fabrication process is relatively complex. Our approach to achieving SDL emission at longer wavelengths is to achieve efficient Raman conversion of the more robust and commercially-tested InGaAs material [2]. More recently we reported Raman conversion of an 1180 nm InGaAs SDL utilizing $KGd(WO_4)_2$ (KGW) to achieve laser operation at 1320 nm with a maximum output power of 2.5 W and diode-to-Stokes efficiency of 4.5% [14].

Diamond has been demonstrated to be a very attractive material for solid-state laser technology over the past decade thanks to its unrivalled high thermal conductivity, robustness, wide optical transparency range, moderate damage threshold and, for Raman lasers, larger Raman gain than established materials such as KGW. Specifically the thermal conductivity, 2000 $Wm^{-1}K^{-1}$, has enabled the demonstration of Raman lasers with good beam quality at high powers [2,15–17]. In this paper we demonstrate, to our knowledge, the longest wavelength achieved by means of intracavity Raman conversion of an SDL using diamond. The coupled cavity of the SDL-pumped Raman laser exploits the large Stokes shift of diamond, 1332 cm^{-1}, to reach laser operation at ~1400 nm in a single Stokes shift.

2. Experiment

The active medium of the SDL used in this work contains ten 5-nm-thick $In_{0.37}Ga_{0.63}As$/GaAs QWs located at the anti-nodes of the optical standing wave with a design wavelength of ~1180 nm. The QWs were monolithically grown on a DBR to provide high reflection (>99.99%) at the fundamental wavelength. The design is similar to that reported in [9,10]. Thermal management was achieved with an intracavity, wedged (<2°), 300-µm-thick diamond heat-spreader (HS), capillary-bonded onto the gain chip. This combination was clamped in a brass mount and water-cooled at 10°C. The external surface of the HS was anti-reflection coated at ~1180 nm.

The SDL gain structure was optically-pumped (see Fig. 1) with a commercial 808-nm fibre-coupled diode laser (fibre core radius of 200 µm) with 400 W of nominal output power. External focusing optics provided a beam focused to a spot radius of ~240 µm at the sample surface with an angle of incidence of ~20°. As the DBR stop-band of the SDL is not spectrally broad enough to provide high reflectivity at the Raman wavelengths, we include the 4-mirror Raman resonator within the fundamental cavity using a plane dichroic mirror (DM) with high reflection (R>99.9%) at >1290 nm and high transmission (T>99%) at <1200 nm. The DM steered the Stokes beam, with a folding angle of <5°, onto the flat output coupler (OC), which had a transmission of ~4% at the Stokes wavelengths. The concave mirrors were coated for high reflection (>99.95%) in the 1150-1770 nm range. Measurement of the emission spectrum was performed using a fibre-coupled optical spectrum analyzer with a resolution limit of 0.05 nm.

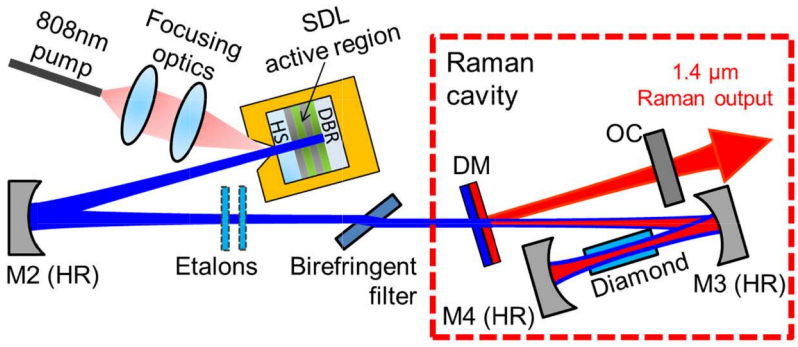

Fig. 1. Scheme of the experimental setup of the SDL-pumped Raman laser. HR: high reflector; DM: dichroic mirror; OC: output coupler; DBR: distributed Bragg reflector; HS: heat-spreader.

Optics EXPRESS

The SDL cavity was designed to produce a beam with a calculated 160-µm spot radius at the surface of the gain chip and a 41 µm beam waist radius at the centre of the 8-mm-long diamond. While all cavity radii were calculated assuming a TEM_{00} mode, the actual beam sizes were larger due to the multi-transverse-mode operation of the SDL. A 4-mm-thick quartz birefringent filter (BRF) was inserted at Brewster's angle in the longest arm of the SDL cavity, outside the Raman resonator, in order to pin the fundamental polarization and to enable tuning of the SDL, and thus tuning of the Raman laser. The 8-mm-long synthetic single-crystal diamond (Element Six Ltd.) was plane-cut for beam propagation along a <110> axis and both end faces were coated for antireflection (R<0.2%) in the 1160-1420 nm range. The diamond was oriented such that the fundamental and Stokes beams were co-polarised along the <111> axis in order to access the highest Raman gain coefficient [18,19]. The concave HR mirrors, labelled as M2, M3 and M4 in Fig. 1, had radius of curvature of 200 mm, 100 mm and 50 mm respectively. The mirror distances were: DBR-M2 = 105 mm, M2-M3 = 450 mm, M3-diamond = 55 mm, diamond-M4 = 48 mm, and M3-DM-OC = 340 mm.

3. Spectral control

Due to the broad spectrum of the output of the free-running SDL and the narrow Raman gain linewidth of the diamond (1.5 cm^{-1} [20]), optimum performance usually requires filtering of the SDL. In addition, an *intracavity* Raman laser setup induces further spectral broadening of the fundamental, which limits the Raman laser performance [2,21,22]. In the Raman laser, the effective Raman gain is reduced by the suboptimal spectral and spatial overlap of the fundamental (the SDL in this case) and Stokes beams in the Raman active medium. Spence [22] suggested that, in the high-dispersion regime, linewidths of the fundamental and the Stokes-shifted modes narrower than the Raman gain linewidth favor operation with higher *effective* Raman gain. To achieve this, we added, within the SDL cavity, uncoated etalon suprasil filters with a range of thicknesses: 50, 100 and 200 µm, with corresponding free spectral ranges, at 1175 nm, calculated to be 9.52 nm, 4.76 nm and 2.38 nm respectively.

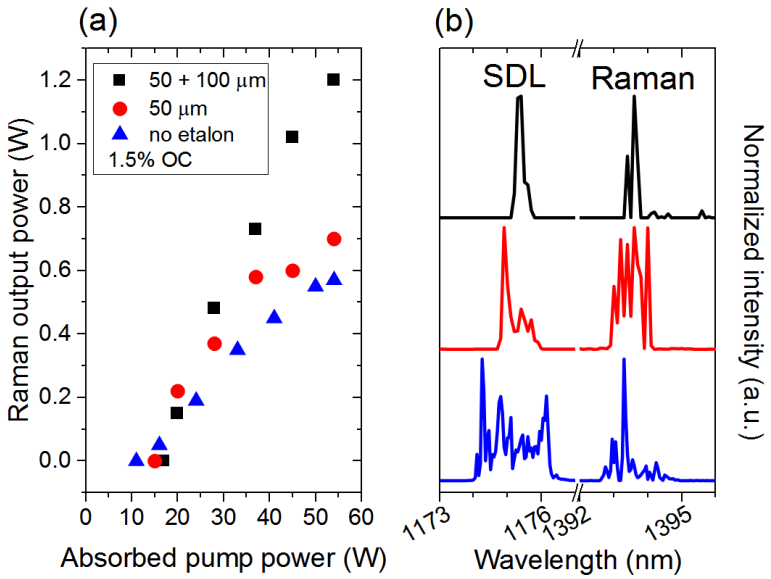

Fig. 2. (a) Raman laser power transfers for output coupler transmission of 1.5% with no etalon (blue triangles), with a 50-µm etalon (red circles), and with both 50 and 100-µm etalons (black squares) in the SDL cavity. (b) The emission spectra of the SDL and Raman lasers at 54 W of absorbed pump power with no etalon (blue), with 50-µm etalon (red), and 50 plus 100-µm etalons (black).

Optics EXPRESS

Figure 2(a) shows the Raman laser power transfer with increasing filtering of the fundamental field: with no etalon, with a 50-µm etalon, and with both a 50 and a 100-µm etalon. At the highest pump power, the maximum output power was, respectively, 0.57, 0.7 and 1.2 W in each case. As can be seen in Fig. 2(b), the additional etalons narrowed the full width at half maximum (FWHM) of the fundamental spectrum from ~2 nm (~10 cm^{-1} FWHM) to <0.2 nm (<1.5 cm^{-1} FWHM).

4. Narrow linewidth operation

With increased output coupling, and the use of two etalons with 50 and 200 µm thickness, the fundamental linewidth was further narrowed. Figure 3(a) shows the Raman laser power transfer characteristic along with, in Fig. 3(b), the SDL and Raman laser emission spectra. The Raman laser emitted up to 2.3 ± 0.1 W for an absorbed diode pump power of 67 W; at this power the intracavity field of the SDL was >420 W. The Raman laser threshold was reached for an absorbed pump power of 20 W. Above threshold, the Raman laser output power increased with the pump power with a slope efficiency of 6%, and in the high-pump power region the intracavity power of the SDL was clamped, as expected for the case of good mode-matching between the fundamental and Raman fields [22]. At high power, the etalon filters allow the fundamental to emit with a single peak (resolution limited) at 1176 nm with 0.14 nm FWHM (1 cm^{-1}) and, consequently, the Stokes-shifted spectrum exhibited a single peak located at 1394.4 nm with a linewidth of 0.1 nm FWHM (0.51 cm^{-1}). This is consistent with previous results that show narrow linewidth operation to be required for efficient pumping of an intracavity diamond Raman laser [2,21].

The Raman laser was not significantly affected by thermal lensing, due to the high thermal conductivity of diamond and the relatively short Raman cavity length. Indeed, according to the approximation given in [23], it can be estimated that the focal length of the thermal lens in the diamond at 2.3 W output power was >1 m.

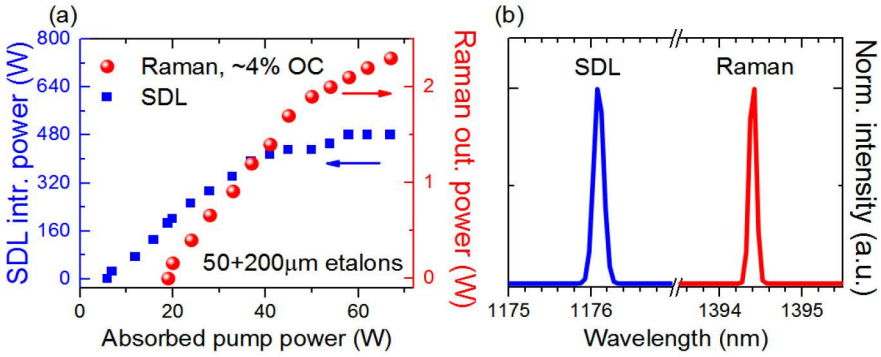

Fig. 3. (a) The Raman laser power transfer for ~4% output coupler transmission with the 50-µm and 200-µm thick etalons (red circles) in the SDL cavity. The SDL intracavity power is also shown (blue squares). (b) The emission spectra of the SDL (blue curve) and Raman laser (red curve) with the 50-µm and 200-µm thick etalons at high Raman power.

The Raman laser polarization was rotated by ~24° with respect to the SDL field, whose polarization was horizontal, pinned by the Brewster's angle of the birefringent filter. Whilst the diamond was oriented such that a <111> axis was parallel to the fundamental field polarization, residual birefringence in the diamond ($\Delta n \sim 3 \times 10^{-6}$), combined with a lack of polarisation constraining element in the Raman laser cavity, cause the Raman laser to oscillate on a polarisation eigenmode that is not aligned to the <111> direction – the direction that might otherwise have been expected to maximise the Raman gain [24]. This residual birefringence is caused by stress induced by dislocations that result from the CVD growth

Optics EXPRESS

process. High quality CVD growth can significantly reduce this birefringence [25], but it remains sufficient to modify the polarisation [24].

Degradation of the SDL beam quality is expected when the intracavity Raman laser reaches threshold [2,21,22]. During Raman conversion, the beam quality factor (M^2) of the Raman laser was 1.4 at high power, while the SDL beam quality worsened from M^2~1.5 to 2.

5. Broad tuning

As shown in Fig. 4(a) tuning of the SDL oscillation wavelength, via rotation of the intracavity BRF, automatically tuned the Raman laser from 1373 to 1415 nm. The tuning range, limited by the free spectral range of the 4-mm-thick BRF, was achieved without etalons (i.e. broad emission) and with 1.5% output coupling. With rotation of the BRF, the SDL demonstrated a relatively smooth tuning curve while the Raman laser tuning curve was discontinuous over the corresponding range. Similar tuning behaviour was observed in a Cr:YAG laser operating in the 1400nm region [26] and was ascribed to varying absorption of water vapour in the atmosphere. The estimated round-trip absorption loss due to water vapour was calculated from the HITRAN database for a 443-mm-long path of air (the laser cavity round trip length) at 1 atm and partial pressure of water vapour of 14 torr, corresponding to our laboratory conditions of 50% relative humidity at 16°C. The resulting spectrum is plotted in Fig. 4(b) showing that the humid air in the enviroment added loss and likely impeded the Raman laser tuning. Intracavity Raman lasers have relatively low gain and therefore they are strongly affected by cavity loss of only a few percent. In our Raman laser resonator, the loss attributed to optics alone (i.e. dielectric coatings and diamond absorption) is calculated to be ~4.9%. A significant drop of performance was observed while tuning the laser to wavelengths at which the water vapour absorption is around 1% or higher.

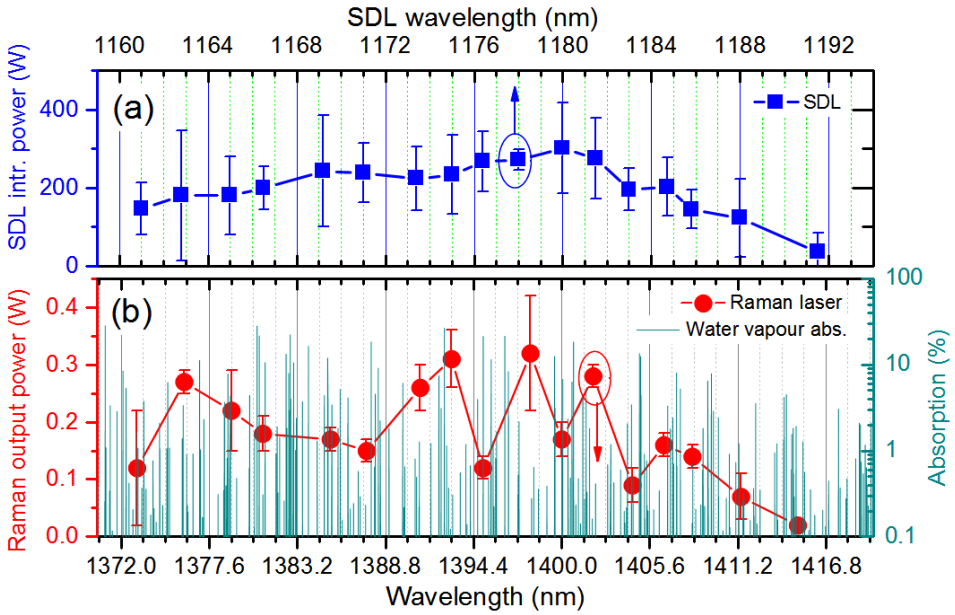

Fig. 4. (a) The tuning range of the intracavity fundamental field (blue squares) for an absorbed pump power of 33 W with 1.5% output coupling of the Raman laser. The straight lines serve as a guide to the eye. (b) The corresponding tuning range of the Raman laser output (red circles) and the estimated round-trip absorption loss due to atmospheric water vapour, calculated for our laboratory conditions using spectroscopic data from the HITRAN database.

Previous demonstrations of SDL-pumped intracavity diamond Raman lasers have reported significantly higher conversion efficiencies, albeit at shorter wavelengths [2,27], achieving up

Optics EXPRESS

to ~14% conversion efficiency. While lower efficiency, as reported here, is expected due to the higher quantum defect, lower SDL efficiency, and lower Raman gain at this wavelength (~11 cm/GW at 1180 nm compared with ~17 cm/GW at 1060 nm [16]), we believe that the performance of this laser could be significantly improved with the implementation of an enclosed, dry air cavity to eliminate water absorption. An alternative solid-state system at this wavelength is a Cr:YAG laser [26,28]; however, they are limited to a few 100 mW at wavelengths around 1.4 μm and require high performance pump lasers, such as Nd:YAG, rather than the relatively low brightness diode laser system used here. Incidentally, a diamond Raman laser has recently been demonstrated to detect water vapour in the 1486 nm region with ~5 nm tuning [3]. An SDL-pumped diamond Raman laser broadly tunable around 1.4 μm (within the'eye-safe' spectral region), may also be attractive for this application. A scheme for intracavity absorption spectroscopy could be envisioned where the Raman laser oscillation wavelength was fixed by a stabilised, narrow-linewidth, tunable SDL.

6. Conclusion

In conclusion, we report a continuous-wave diamond Raman laser intracavity pumped by an InGaAs-based semiconductor disk laser. The laser emitted at ~1.4 μm, tunable over >40 nm from 1373 to 1415 nm via rotation of a birefringent filter located in the SDL resonator. This is the longest wavelength so far reported from a SDL-pumped diamond Raman laser. The Raman laser power was maximized via the use of two intracavity suprasil etalons with 200 and 50 μm thickness to narrow the fundamental mode, reaching up to 2.3 W of output power (3.4% of diode-to-Stokes optical conversion efficiency). The Raman laser also operated with a narrow linewidth (<0.1 nm FWHM) and good beam quality (M^2 = 1.4) at high power.

Funding

UK EPSRC Challenging Engineering Award (EP/I022791/1); ERC DiaL Grant (278389) Fraunhofer UK Ltd and the Royal Academy of Engineering. J.-P. Penttinen and M. Guina acknowledge financial support from Academy of Finland project QUBIT (278338) and TEKES project "ReLase" (40016/14).

Acknowledgments

The data sets related to this publication have been made available at http://dx.doi.org/10.15129/f123cf38-3ab2-48d6-b919-e2e310abaee3.